



Cite this: *Chem. Commun.*, 2014, 50, 15995

Received 6th August 2014,
Accepted 7th November 2014

DOI: 10.1039/c4cc06159d

www.rsc.org/chemcomm

The electrocatalytic proton reduction activity of a Ni bis(diphosphine) (NiP) and a cobaloxime (CoP) catalyst has been studied in water in the presence of the gaseous inhibitors O₂ and CO. CoP shows an appreciable tolerance towards O₂, but its activity suffers severely in the presence of CO. In contrast, NiP is strongly inhibited by O₂, but produces H₂ under high CO concentrations.

The implementation of an artificial photosynthetic system would offer a sustainable route to clean and storable energy.¹ This process could generate H₂ fuel, or a gas mixture of H₂ and CO, known as syngas, which can be used to produce long-chain hydrocarbons or methanol.² Proton reduction catalysts are an integral part of either system and have consequently generated considerable research interest.³

Inhibitor tolerance under real-world operating conditions is a vital trait for a proton reduction catalyst, but has received relatively little attention to date. Depending on the intended use of a system, proton reduction catalysts could be exposed to large amounts of O₂ (through water splitting) or CO (CO₂ splitting). Trace amounts of such inhibitors typically poison the most active H₂ evolution catalysts, such as platinum⁴ and H₂-producing enzymes (hydrogenases).^{5,6}

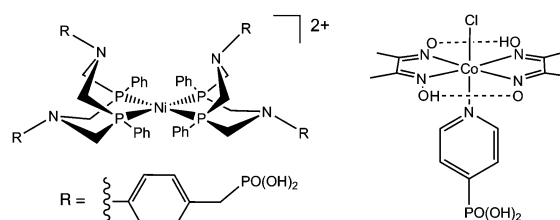
Molecular synthetic catalysts offer an alternative route to proton reduction^{7–9} and it has recently emerged that some molecular catalysts are tolerant towards O₂ in aqueous solution. This observation has prompted a number of contemporary studies into H₂ evolution under aerobic conditions. Co-based complexes make up the majority of these O₂ tolerant species; cobaloximes were the first earth-abundant catalysts shown to be functional under air,¹⁰ followed by a Co-corrole catalyst¹¹ and a Co-microperoxidase.¹²

Recently, a rationally designed bis(1,5-R'-diphospho-3,7-R''-diazacyclooctane)Ni catalyst from DuBois and co-workers has set a new benchmark for H₂ production activity.¹³ Derivatives of

this Ni catalyst have since been able to generate considerable amounts of H₂ from aqueous solutions,^{14,15} an important step in the development of water-splitting systems.¹⁶ However, inhibition remains unexplored for this promising type of catalyst.

Herein, we have used a water-soluble Ni bis(diphosphine) catalyst (NiP),¹⁴ as well as a cobaloxime (CoP)¹⁷ (Scheme 1) to study inhibition of catalytic proton reduction activity by O₂ and CO. Inhibition prevents catalysts from undergoing redox reactions essential for catalytic H₂ evolution, therefore electrochemical analysis was fundamental to this work. Cyclic voltammetry has been used to monitor changes in the redox and electrocatalytic activity of CoP and NiP under atmospheres of O₂ or CO on a short time-scale and controlled potential electrolysis (CPE) combined with H₂ analysis has explored the inhibition of H₂-evolution activity over longer periods of time. Spectroelectrochemistry allowed the potential-dependent formation of inhibited species to be analysed.

Cyclic voltammograms (CVs) were recorded on a glassy carbon disk electrode (0.07 cm²) at 100 mV s⁻¹ using conditions optimised for high catalyst activity (pH 4.5 for NiP¹⁴ and pH 7 for CoP^{17,18}). Initial studies into H₂ inhibition (up to 100% H₂) showed no product inhibition for NiP and CoP (Fig. S1, ESI†), allowing the effect of other inhibiting gases to be established during proton reduction. Fig. 1a and b display CVs of NiP and CoP under inert and aerobic atmospheres. Irreversible O₂ reduction occurs at $E_p = -0.5$ V vs. normal hydrogen electrode (NHE) at the glassy carbon electrode, resulting in an increased



Scheme 1 Chemical structure of Ni and Co catalysts used in this study. Both compounds contain phosphonic acid moieties to allow dissolution in aqueous media and the Ni and Co catalysts have therefore been labelled as NiP and CoP, respectively.

Christian Doppler Laboratory for Sustainable SynGas Chemistry,
Department of Chemistry, University of Cambridge, Lensfield Road,
Cambridge CB2 1EW, UK. E-mail: reisner@ch.cam.ac.uk

† Electronic supplementary information (ESI) available: Experimental details, Tables S1 and S2 and Fig. S1–S6. See DOI: 10.1039/c4cc06159d



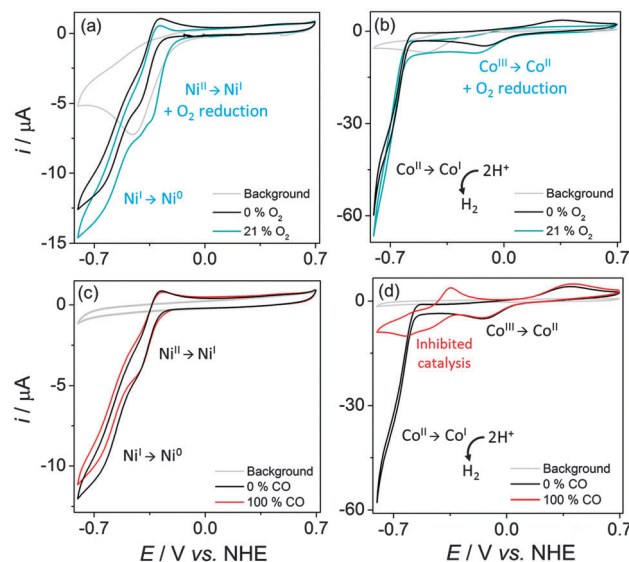


Fig. 1 CVs (100 mV s^{-1} on a glassy carbon disk electrode) of (a) and (c) **NiP** (1 mM) in citrate buffer (0.1 M, pH 4.5) and (b) and (d) **CoP** (1 mM) in triethanolamine- Na_2SO_4 (0.1 M each, pH 7) in atmospheres of 100% N_2 , 21% O_2 (air) and 100% CO. The grey background traces were generated from air or CO saturated electrolyte solutions without catalyst.

current response in air, which must be taken into account in this analysis.

Under inert conditions, the CV of **NiP** displays two waves at potentials more negative than -0.3 V vs. NHE, which have been assigned to the reduction of Ni^{II} to Ni^{I} followed by Ni^{I} to a formal Ni^{0} .¹⁴ The CV lacks a strong catalytic wave, presumably because most of the proton reduction by **NiP** occurs after Ni^{0} has diffused away from the electrode-solution interface.¹⁹ The CV trace recorded under 21% O_2 (blue trace in Fig. 1a) shows almost no change compared to inert conditions when the O_2 reduction current (grey trace) is disregarded. The degree of inhibition could not be obtained from the CVs due to the weak catalytic wave of **NiP**. CPE subsequently confirmed the catalytic proton reduction activity of **NiP** and was used to monitor the degree of O_2 inhibition (see below).

The analogous CVs of **CoP** are displayed in Fig. 1b. Under inert conditions, the cobaloxime first undergoes a reduction from Co^{III} to Co^{II} , followed by a strong catalytic wave at an onset potential of -0.6 V , as Co^{II} is reduced to Co^{I} and proton reduction catalysis is initiated.²⁰ Under 21% O_2 , the proton reduction wave of **CoP** is almost identical suggesting high catalytic activity under air. The O_2 reduction wave at -0.5 V however overlaps with the $\text{Co}^{\text{III}}/\text{Co}^{\text{II}}$ reduction wave around -0.2 V vs. NHE suggesting that Co^{II} may be reducing dissolved O_2 . Catalytic H_2 generation is thus in competition with oxidation of the reduced Co species (Co^{II} and Co^{I}) by O_2 . This was confirmed through analysis of the $\text{Co}^{\text{III}}/\text{Co}^{\text{II}}$ redox couple in air, which showed a loss of the anodic Co^{II} to Co^{III} wave due to prior oxidation of Co^{II} by O_2 (Fig. S2, ESI†).^{21,22}

CVs of **NiP** and **CoP** under a CO atmosphere are presented in Fig. 1c and d. Assuming saturation of water with CO at a concentration of 1 mM,²³ the concentration of CO is comparable to the catalyst concentration. The reduction waves of **NiP** do not show any

significant changes upon introduction of 100% CO (Fig. 1c). The cobaloxime demonstrates a low tolerance towards CO compared to the Ni bis(diphosphine) catalyst (see results from CPE below). CVs of **CoP** under N_2 and CO have identical $\text{Co}^{\text{III}}/\text{Co}^{\text{II}}$ reduction ($E_p = -0.14 \text{ V}$) and oxidation ($E_p = +0.4 \text{ V}$) waves under N_2 and CO (Fig. 1d). Upon reduction of Co^{II} to Co^{I} however, the proton reduction activity is no longer observed as the cobaloxime is inhibited.

A long-term, more quantitative measure of inhibition was achieved through CPE, which analysed changes in the H_2 produced by both catalysts. CPE was particularly important for the study of **NiP**, where little catalysis was observed in the CVs. A glassy carbon rod (approximately 2 cm^2) was held at -0.4 V vs. NHE for **NiP** and -0.7 V vs. NHE for **CoP**, whilst stirring under different atmospheres. The H_2 produced was detected by headspace gas chromatography (Fig. 2 and Table S1, ESI†). Faradaic efficiencies were calculated and gave respectable numbers for molecular catalysts held at such low overpotentials ($>65\%$ in all cases).

CPE of **CoP** for 15 min in the presence of air illustrated the tolerance of cobaloximes to O_2 . The CPE timescale was kept short to avoid the formation of heterogeneous catalysts on the electrode surface.²⁴ A drop in proton reduction activity was seen under air compared to N_2 , due to increasing catalyst oxidation by O_2 , yet the catalyst still retained appreciable activity. The Faradaic efficiency similarly drops due to increasing O_2 reduction by both the electrode and catalyst. The remarkable tolerance towards O_2 has been attributed previously to the abundance of aqueous protons over O_2 in the electrochemical cell¹⁰ (0.3 mM O_2 under aerobic conditions) combined with the low affinity of the cobaloxime for forming irreversible inhibition products with O_2 . The reduction of oxygen presumably leads to the production of water in a similar manner to oxygen tolerant hydrogenases,²⁵ allowing parallels to be drawn between these systems.

The activity of **NiP** was much more sensitive to O_2 . Despite the apparent tolerance displayed in the CV (Fig. 1a), 60 min of CPE under air at -0.4 V vs. NHE produced only negligible amounts of H_2 . The level of H_2 recorded was comparable to the small quantity produced by the glassy carbon rod electrode without a catalyst. This complete inhibition of **NiP** suggests that an oxidised,

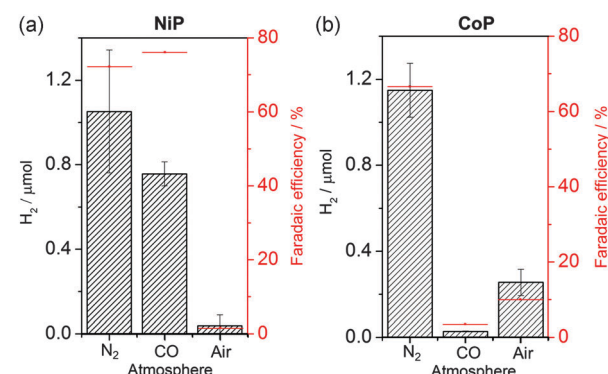


Fig. 2 Electrocatalytic production of H_2 (black bars) and Faradaic efficiency (red lines) from CPE of (a) **NiP** (0.5 mM) in citrate buffer (0.1 M, pH 4.5) at -0.4 V vs. NHE for 60 min and (b) **CoP** (0.5 mM) in triethanolamine- Na_2SO_4 (0.1 M each, pH 7) at -0.7 V vs. NHE for 15 min.

inactive inhibition product is forming. Studies into O_2 reduction by similar structures identified the formation of inactive phosphine oxides at low Ni oxidation states²⁶ and gives a possible explanation for the observed inhibition on the CPE timescale. It may thus be concluded that in order to prevent O_2 inhibition it is important to avoid ligand functionality that is susceptible to irreversible oxidation, such as phosphines. Upon repurging with N_2 72% of the initial H_2 production rate was observed, as the catalyst molecules that are not reduced during CPE are relatively O_2 stable in the bulk solution.

On the other hand, **NiP** is completely tolerant to CO. CPE produced similar levels of H_2 under both 100% CO and 100% N_2 (Fig. 2a). The tolerance of **NiP** towards CO is remarkable considering the strongly inhibitive effect of CO on most catalytic surfaces, such as Pt. Experiments into Pt inhibition showed that the H_2 produced by a Pt disk electrode held at -0.4 V vs. NHE for 15 min produced minimal H_2 under CO (Fig. S3 and Table S2, ESI[†]). The Ni bis(diphosphine) structure is designed to mimic hydrogenase enzymes²⁷ and the coordination sphere of a similar Ni bis(diphosphine) complex has previously demonstrated rapid reversible CO binding.²⁸ This may prevent the CO from having a significant inhibiting impact on proton reduction in a manner much akin to the few reported CO-tolerant hydrogenases.^{29,30}

This result is in contrast to **CoP**, which exposes an easily accessible coordination site in its catalytic cycle,³¹ and is consequently susceptible to CO binding. **CoP** was completely inhibited by CO; 15 min of CPE at -0.7 V vs. NHE produced minimal H_2 . However, CO inhibition of **CoP** was completely reversible and 100% of the electroactivity could be regained after purging with N_2 (see Fig. S4, ESI[†]). The inhibition of the aforementioned Pt disk was irreversible and could not be reactivated with a N_2 purge (Fig. S3, ESI[†]).

IR-spectroelectrochemical studies were carried out to gain a better understanding of cobaloxime inhibition. Using a spectroelectrochemical cell (Pt working and counter electrodes, Ag wire reference)³² IR-spectra were taken of $[CoCl(dimethylglyoximato)_2(4-methoxypyridine)]$ under CO at a range of potentials (Fig. 3a). The methoxypyridine analogue of **CoP** was used due to its higher solubility in MeOH.³¹ UV-visible spectra were recorded to follow the oxidation state change of the complex (Fig. 3b).

Upon reaching potentials at which Co^I forms in the UV-visible spectra³³ (-0.65 V vs. Ag/Ag^+) a peak is observed in the IR spectra at 1970 cm^{-1} , which is the expected region for a cobaloxime-carbonyl species.³⁴ This peak has been assigned to substitution of the labile axial pyridine for CO at the low Co oxidation state.³⁵ No carbonyl peak was observed under an atmosphere of N_2 (Fig. S5, ESI[†]). Electron withdrawing axial ligands, such as CO, decrease cobaloxime proton reduction activity by reducing the basicity of the intermediate Co-H that forms in the catalytic cycle,³¹ thereby explaining the loss of catalytic activity.

No Ni-carbonyl peaks are present in the IR spectra of **NiP** under a CO atmosphere at any potential applied (Fig. 3c). The UV-visible spectroelectrochemistry displays bands that have been assigned to $Ni^{II}/Ni^{I}/Ni^0$ from -0.4 to -1 V vs. Ag/Ag^+ (Fig. 3d). The Ni^{II} state has a band at 520 nm corresponding to a pink color that is lost upon formation of Ni^I . The Ni^I state shows little absorption

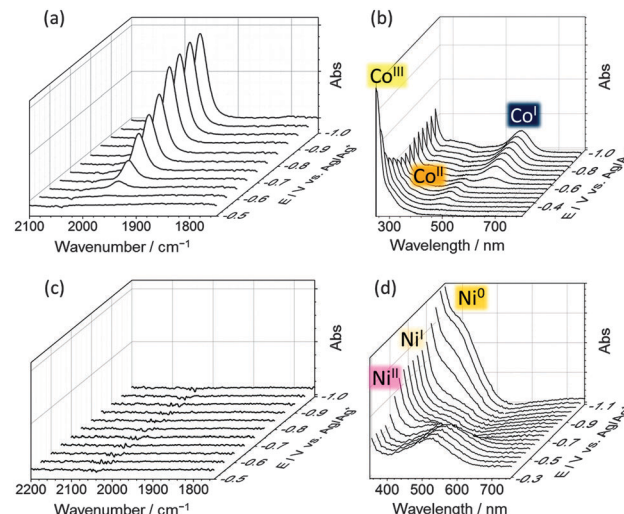


Fig. 3 (a) and (c) IR-spectroelectrochemical traces of $[CoCl(dimethylglyoximato)_2(4\text{-methoxypyridine})]$ (~ 5 mM) and **NiP** (1.25 mM), respectively. (b) and (d) UV-visible spectroelectrochemical traces of $[CoCl(dimethylglyoximato)_2(4\text{-methoxypyridine})]$ (0.25 mM) and **NiP** (0.25 mM), respectively. All spectra were taken in the presence of tetrabutylammonium bromide (0.3 M) in MeOH under an atmosphere of CO at increasingly negative potentials.

in the visible region but a shift in the UV peak at 250 nm occurs (Fig. S6, ESI[†]). Upon formation of Ni^0 a yellow color is seen as suggested by the shoulder in the UV-vis spectrum at 400 nm and previous accounts.³⁶ The lack of Ni-carbonyl peak across these oxidation states illustrates the tolerance of the Ni bis(diphosphine) to carbonyl binding and explains the sustained proton reduction activity under these conditions.

In summary, Ni bis(diphosphine) and cobaloxime catalysts are widely used state-of-the-art catalysts for the reduction of aqueous protons. Our study demonstrates their distinct tolerance to well-known gaseous inhibitors and illustrates the ways in which molecular catalysts can be designed to fulfill the requirements of a specific system. **NiP** shows unprecedented activity under CO and can therefore be employed in systems where CO is present, such as syngas generating devices. CO reversibly inhibits **CoP** due to the formation of an inactive Co-CO species as confirmed by IR-spectroelectrochemistry. On the other hand, the cobaloxime showed appreciable tolerance towards O_2 , whereas the Ni bis(diphosphine) complex lost all activity. Ongoing studies seek to gain a more detailed understanding of the relationship between the structure of a catalyst and its resultant tolerance to inhibition.

Financial support from the EPSRC (EP/H00338X/2), the Christian Doppler Research Association (Austrian Federal Ministry of Science, Research and Economy and National Foundation for Research, Technology and Development), and the OMV Group is gratefully acknowledged.

Notes and references

- 1 N. S. Lewis and D. G. Nocera, *Proc. Natl. Acad. Sci. U. S. A.*, 2006, **103**, 15729–15735.
- 2 M. E. Dry, *Catal. Today*, 2002, **71**, 227–241.
- 3 P. Du and R. Eisenberg, *Energy Environ. Sci.*, 2012, **5**, 6012–6021.
- 4 N. P. Dasgupta, C. Liu, S. Andrews, F. B. Prinz and P. Yang, *J. Am. Chem. Soc.*, 2013, **135**, 12932–12935.



5 E. Reisner, *Eur. J. Inorg. Chem.*, 2011, 1005–1016.

6 F. A. Armstrong, N. A. Belsey, J. A. Cracknell, G. Goldet, A. Parkin, E. Reisner, K. A. Vincent and A. F. Wait, *Chem. Soc. Rev.*, 2009, **38**, 36–51.

7 T. S. Teets and D. G. Nocera, *Chem. Commun.*, 2011, **47**, 9268–9274.

8 W. T. Eckenhoff and R. Eisenberg, *Dalton Trans.*, 2012, **41**, 13004–13021.

9 H. I. Karunadasa, E. Montalvo, Y. Sun, M. Majda, J. R. Long and C. J. Chang, *Science*, 2012, **335**, 698–702.

10 F. Lakadamyali, M. Kato, N. M. Muresan and E. Reisner, *Angew. Chem., Int. Ed.*, 2012, **51**, 9381–9384.

11 B. Mondal, K. Sengupta, A. Rana, A. Mohammed, M. Botoshansky, S. G. Dey, Z. Gross and A. Dey, *Inorg. Chem.*, 2013, **52**, 3381–3387.

12 J. G. Kleingardner, B. Kandemir and K. L. Bren, *J. Am. Chem. Soc.*, 2014, **136**, 4–7.

13 M. L. Helm, M. P. Stewart, R. M. Bullock, M. Rakowski DuBois and D. L. DuBois, *Science*, 2011, **333**, 863–866.

14 M. A. Gross, A. Reynal, J. R. Durrant and E. Reisner, *J. Am. Chem. Soc.*, 2014, **136**, 356–366.

15 A. Dutta, S. Lense, J. Hou, M. H. Engelhard, J. A. S. Roberts and W. J. Shaw, *J. Am. Chem. Soc.*, 2013, **135**, 18490–18496.

16 J. R. McKone, N. S. Lewis and H. B. Gray, *Chem. Mater.*, 2014, **26**, 407–414.

17 F. Lakadamyali and E. Reisner, *Chem. Commun.*, 2011, **47**, 1695–1697.

18 P. Du, K. Knowles and R. Eisenberg, *J. Am. Chem. Soc.*, 2008, **130**, 12576–12577.

19 C. Costentin, S. Drouet, M. Robert and J.-M. Savéant, *J. Am. Chem. Soc.*, 2012, **134**, 11235–11242.

20 J. L. Dempsey, B. S. Brunschwig, J. R. Winkler and H. B. Gray, *Acc. Chem. Res.*, 2009, **42**, 1995–2004.

21 M. Shamsipur, A. Salimi, H. Haddadzadeh and M. F. Mousavi, *J. Electroanal. Chem.*, 2001, **517**, 37–44.

22 G. N. Schrauzer, *Angew. Chem., Int. Ed.*, 1976, **15**, 417–426.

23 P. Scharlin, R. Battino, E. Silla, I. Tuñón and J. L. Pascual-Auir, *Pure Appl. Chem.*, 1998, **70**, 1895–1904.

24 S. Cobo, J. Heidkamp, P.-A. Jacques, J. Fize, V. Fourmond, L. Guetaz, B. Jousselme, V. Ivanova, H. Dau, S. Palacin, M. Fontecave and V. Artero, *Nat. Mater.*, 2012, **11**, 802–807.

25 W. Lubitz, H. Ogata, O. Rüdiger and E. Reijerse, *Chem. Rev.*, 2014, **114**, 4081–4148.

26 J. Y. Yang, R. M. Bullock, W. G. Dougherty, W. S. Kassel, B. Twamley, D. L. DuBois and M. Rakowski DuBois, *Dalton Trans.*, 2010, **39**, 3001–3010.

27 A. D. Wilson, R. H. Newell, M. J. McNevin, J. T. Muckerman, M. Rakowski DuBois and D. L. DuBois, *J. Am. Chem. Soc.*, 2006, **128**, 358–366.

28 A. D. Wilson, K. Fraze, B. Twamley, S. M. Miller, D. L. DuBois and M. Rakowski DuBois, *J. Am. Chem. Soc.*, 2008, **130**, 1061–1068.

29 K. A. Vincent, J. A. Cracknell, O. Lenz, I. Zebger, B. Friedrich and F. A. Armstrong, *Proc. Natl. Acad. Sci. U. S. A.*, 2005, **102**, 16951–16954.

30 X. Luo, M. Brugna, P. Tron-Infossi, M. T. Giudici-Orticoni and É. Lojou, *J. Biol. Inorg. Chem.*, 2009, **14**, 1275–1288.

31 D. W. Wakerley and E. Reisner, *Phys. Chem. Chem. Phys.*, 2014, **16**, 5739–5746.

32 M. Krejčík, M. Daněk and F. Hartl, *J. Electroanal. Chem.*, 1991, **317**, 179–187.

33 N. M. Muresan, J. Willkomm, D. Mersch, Y. Vaynzof and E. Reisner, *Angew. Chem., Int. Ed.*, 2012, **51**, 12749–12753.

34 X. Hu, B. M. Cossairt, B. S. Brunschwig, N. S. Lewis and J. C. Peters, *Chem. Commun.*, 2005, 4723–4725.

35 T. M. McCormick, Z. Han, D. J. Weinberg, W. W. Brennessel, P. L. Holland and R. Eisenberg, *Inorg. Chem.*, 2011, **50**, 10660–10666.

36 E. S. Wiedner, J. Y. Yang, S. Chen, S. Raugei, W. G. Dougherty, W. S. Kassel, M. L. Helm, R. M. Bullock, M. Rakowski DuBois and D. L. DuBois, *Organometallics*, 2012, **31**, 144–156.

